doi:10.1006/jmbi.2000.4123 available online at http://www.idealibrary.com on IDEAL® *J. Mol. Biol.* (2000) **302**, 1139–1151

JMB

Structural Analysis of the Transcriptional Activation Region on Fis: Crystal Structures of Six Fis Mutants with Different Activation Properties

Yi-Sheng Cheng[1,2], Wei-Zen Yang[2], Reid C. Johnson[3] and Hanna S. Yuan[1,2,4]*

[1]*Graduate Institute of Life Science, National Defense Medical Center, Taipei, Taiwan Republic of China*

[2]*Institute of Molecular Biology Academia Sinica, Taipei Taiwan, 11529, Republic of China*

[3]*Department of Biological Chemistry and Molecular Biology Institute, University of California, Los Angeles CA 90095-1737, USA*

[4]*Institute of Biochemistry National Taiwan University Taipei, Taiwan, Republic of China*

**Corresponding author*

The Fis protein regulates gene expression in *Escherichia coli* by activating or repressing transcription of a variety of genes. Fis can activate transcription when bound to DNA upstream of the RNA-polymerase-binding site, such as in the *rrnB* P1 promoter, or when bound to a site overlapping the −35 RNA polymerase binding site, such as in the *proP* P2 promoter. It has been suggested that transcriptional activation in both promoters results from interactions between specific amino acids within a turn connecting the B and C helices (the BC turn) in Fis and the C-terminal domain of the α-subunit of RNA polymerase (αCTD of RNAP). Here, crystal structures of six Fis BC turn mutants with different transcriptional activation properties, Q68A, R71Y, R71L, G72A, G72D and Q74A, were determined at 1.9 to 2.8 Å resolution. Two of these mutants, R71Y and R71L, crystallized in unit cells which are different from that of wild-type Fis, and the structure of R71L offers the most complete Fis model to date in that the extended structure of the N-terminal region is revealed. The BC turn in all of these mutant structures remains in a nearly identical γγ β-turn conformation as present in wild-type Fis. Analyses of the molecular surfaces of the transactivation region of the mutants suggest that several residues in or near the BC turn, including Gln68, Arg71, Gly72 and Gln74, form a ridge that could contact the αCTD of RNAP on one side. The structures and biochemical properties of the mutants suggest that Arg71 is the most critical residue for contacting RNAP within this ridge and that the glycine at position 72 helps to stabilize the structure.

Keywords: Fis; transcriptional activation; RNA polymerase αCTD; protein-protein interaction; β-turn structure

Introduction

Transcription in *Escherichia coli* is catalyzed by the multisubunit enzyme RNA polymerase (RNAP), which consists of a β, β′ two α, and one of a number of alternative σ-subunits. Current evidences indicate that transcription factors interact with each of the four RNAP subunits to regulate transcription, and the carboxyl-terminal domain of the α-subunit (αCTD) is one of the major interacting targets for transcriptional factors (Hochschild & Dove, 1998; Ishihama, 1993; Rhodius & Busby, 1998). The Fis protein is an example of a transcription factor that has been shown to stimulate transcription *via* the αCTD (Bokal *et al.*, 1997; McLeod *et al.*, 1999).

Originally, Fis was identified by its ability to stimulate site-specific DNA inversion in prokaryotic DNA inversion systems (Johnson *et al.*, 1986; Koch & Kahmann, 1986). However, it is now apparent that Fis functions more generally as a global transcription factor that positively or negatively regulates transcription of many genes in enteric bacteria (Champagne & Lapointe, 1998; Falconi *et al.*, 1996; Gonzalez-Gil *et al.*, 1996; Green *et al.*,

Abbreviation used: αCTD, carboxy-terminal domain of the α-subunit.

E-mail address of the corresponding author: hanna@sinica.edu.tw

0022-2836/00/051139–13 $35.00/0

1996; Lazarus & Travers, 1993; Nilsson *et al*., 1990; Ross *et al*., 1990; Wu *et al*., 1998; Xu & Johnson, 1995a). Under nutrient rich conditions, Fis is the most abundant transcriptional regulator in the cell (Ali Azam *et al*., 1999; Ball *et al*., 1992; Osuna *et al*., 1995). However, cellular levels of Fis are much lower under poor growth conditions and are undetectable in stationary phase. The growth rate and growth phase dependent regulation appears to have been an important factor in the recruitment of Fis as a specific activator or repressor of a wide variety of genes.

Crystal structures of wild-type and mutant Fis dimers (see Figure 1) have revealed an α-helical core consisting of four helices (A-D) per subunit (Kostrewa *et al*., 1991; Yuan *et al*., 1991). The C-terminal C and D helices form a helix-turn-helix DNA-binding motif that is responsible for site-specific DNA binding. The unusually close spacing between the DNA recognition helices in the dimer contributes to the prominent DNA bending induced upon Fis-DNA binding. In addition, DNA flanking the 15 bp degenerate core binding site can interact with the sides of Fis, particularly at Arg71, to create additional curvature (Pan *et al*., 1996). A flexible β-hairpin arm that extends from the N termini of each subunit is essential for controlling site-specific DNA inversion (Safo *et al*., 1997). However, the amino acid residues within this region appear to have no role in regulating transcription.

Fis can activate transcription when bound upstream of the core promoter region (class I position) or when overlapping the −35 region of the RNA-polymerase-binding site (class II position) (see Figure 2). In both the *rrnB* P1 promoter (class I) and the *proP* P2 promoter (class II), extensive mutational analysis has defined a small group of amino acid residues that are required on one of the Fis dimer subunits for activation (Bokal *et al*., 1997; Gosink *et al*., 1996; McLeod *et al*., 1999). These amino acid residues are localized to a small region near the C terminus of helix B (Gln68), the turn between helices B and C (Arg71, Gly72 and Asn73) and the beginning of helix C (Gln74). Amino acid substitutions at these residues have varying effects on transcriptional activation and some also affect DNA binding. Fis and the sigma-70 form of holoenzyme at *rrnB* P1 or the sigma-38 form of holoenzyme at *proP* P2 bind cooperatively (Bokal *et al*., 1995; Xu & Johnson, 1997), and where tested, mutants within the BC turn of Fis perturb this interaction. Moreover, Fis-activation of *rrnB* and *proP* also requires the presence of the αCTD,

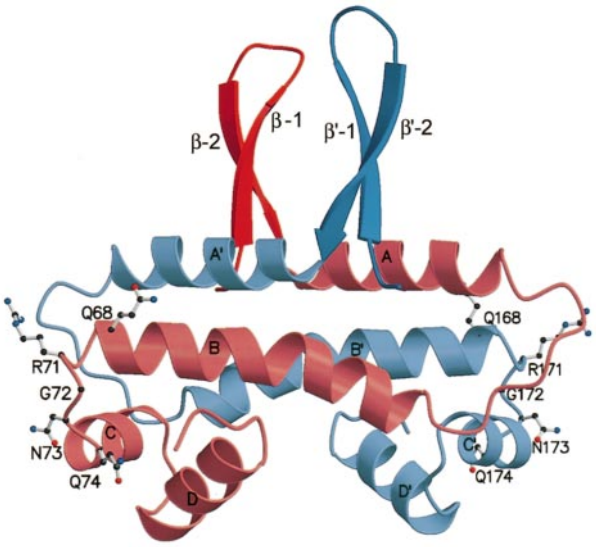

Figure 1. Ribbon model of the Fis dimer. The crystal structures of wild-type Fis (residues 26 to 98) and K36E (residues 10 to 25) were combined to give a more complete model of Fis. The core helix structure of the wild-type Fis dimer is shown in pink and light blue, and the N-terminal β-hairpin arms from K36E are shown in red and blue. The two Fis subunits are numbered from 1 to 98, and 101 to 198, respectively. The side-chains of several residues in the BC turn, including Gln68, Arg71, Gly72, Asn73, and Gln74, that show decreased transcription activity at the *rrnB* P1 or *proP* P2 promoters are displayed as ball-and-stick models.

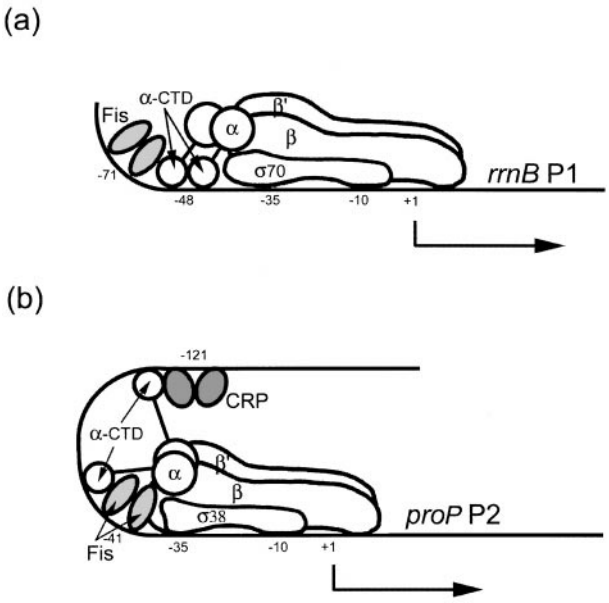

Figure 2. A cartoon model of Fis functioning as a transcriptional activator at two different promoters. (a) In the *rrnB* P1 promoter, Fis functions as a class I transcriptional activator binding upstream of the binding site for the sigma-70 form of RNA polymerase (RNAP) (Bokal *et al*., 1997). (b) In the *proP* P2 promoter, Fis functions as a class II transcriptional activator binding at the site overlapping the −35 binding site of the sigma-38 form of RNAP (Xu & Johnson, 1995b). CRP (catabolite gene activator) co-activates the *proP* P2 promoter with Fis (McLeod *et al*., 2000), and these two transcription activators are shaded to distinguish them from the unshaded RNA polymerase.

suggesting that a Fis-αCTD interaction mediates the stimulation under both promoter configurations (Bokal *et al*., 1997; McLeod *et al*., 1999). The precise region on the αCTD that is contacted by Fis is currently under investigation.

The strongest transcription phenotypes are generated by mutations at residues 71 and 72 within the short constrained loop connecting the B and C α-helices. As discussed below, these residues adopt a left handed α-helical configuration raising the possibility that substitutions within this region may have structural consequences that could contribute to their altered activities. To directly investigate this possibility, we determined the crystal structures of a leucine and tyrosine substitution at Arg71, which have opposite effects on transcription, and an alanine and aspartic acid substitution at Gly72, both of which result in severe defects in transcription. In addition, the structural consequences of alanine replacements of Gln68 and Gln74, which also interfere with transcriptional activation, were examined. We find that while the side-chain differences are apparent, the backbone structures of the BC turn in these mutants are almost identical to that of the wild-type Fis. A comparison of the molecular surfaces of the transactivation regions in these mutants leads to a model in which one side of a ridge containing Gln68, Arg71, Gly72 and possibly Gln74 forms a target for interaction with the αCTD of RNAP.

Results and Discussion

Properties of Fis BC turn mutants: transcription activation, DNA binding, DNA bending, and thermal stability

The Fis BC turn connecting the C terminus of the B-helix (Thr70) and the N terminus of the C-helix (Gln74) consists of residues 71 to 73 (Arg71, Gly72 and Asn73). Table 1 summarizes the transcriptional activation and DNA binding properties of mutants within this region. The transcriptional activation properties of these mutants are obtained from *in vivo* and *in vitro* measurements at *rrnB* P1 (Bokal *et al*., 1997; Gosink *et al*., 1996; S. Aiyar & R. Gourse, personal communication) and *proP* P2 (McLeod *et al*., 1999). Alanine substitutions at Tyr69 and Thr70 did not significantly affect transcriptional activation and thus are not included in the Table. The melting points of the mutants were measured in this study by thermal denaturation of Fis proteins as monitored by circular dichroism. Table 1 also summarizes the stability of Fis-DNA complexes as measured by the dissociation rates between Fis and DNA, and DNA

Table 1. Thermal stability, transcriptional activity, and DNA-binding properties of Fis BC turn mutants

			Fis-DNA[d]		
Mutant[a]	*T*m (°C)[b]	Transcriptional activation[c]	*K*d (nM)	Stability	Bending
WT	57.8	High	3	Stable	WT
Q68A*	62.9	Low	3	Stable	WT
R71A	57.7	Very low	3	Unstable	Reduced
R71Y*	54.3	High	3	Unstable	Reduced
R71L*	58.7	Very low	4	ND	More reduced
R71D	61.0	Very low	3	Unstable	Reduced
R71K	ND	Very low	3	Stable	WT
G72A*	49.1	Very low	4	Stable	WT
G72D*	42.4	Very low	3	ND	ND
N73A	ND	Very low	30	Unstable	Reduced
N73S	ND	Variable	4	Unstable	Slightly reduced
Q74A*	62.4	Low	3	Unstable	WT

[a] The crystal structures of the mutants denoted with asterisks were determined in this study.

[b] Thermal denaturation transition midpoints of the proteins were measured by CD at 220 nm. ND indicates not determined.

[c] Transcriptional activation properties of the mutants are from *in vivo* and *in vitro* measurements at *proP* P2 (McLeod *et al*., 1999) and *rrnB* P1 (Gosink *et al*., 1996; Bokal *et al*., 1997; S. Aiyar & R. Gourse, personal communication). Where data are available, the relative activities of the mutants at both promoters are very similar. Low indicates 20-40% of wild-type activity, very low is <10% of wild-type activity, variable (N73S) indicates that the low activity under standard conditions *in vitro* can be increased to about 60% of wild-type in the presence of large amounts of protein.

[d] DNA-binding properties of the Fis DNA complex. K_d values represent binding at *proP* Fis site I (McLeod *et al*., 1999); where tested, relative affinities at the *rrnB* Fis site I are similar (Gosink *et al*., 1996; Bokal *et al*., 1997). The stability of Fis-DNA complexes was determined by measuring the rate of dissociation of a preformed complex after addition of excess specific binding sites (Pan *et al*., 1996; McLeod *et al*., 1999; S. McLeod & R.C.J., unpublished results). ''Stable'' indicates a dissociation rate similar to that of wild-type Fis (e.g., 50% of the preformed Fis-DNA complex remained 30 minutes after competitor added) and ''unstable'' indicates the mutant Fis-DNA complex dissociated faster than that of the wild-type Fis-DNA complex (<50% of the preformed Fis-DNA complex remained five minutes after competitor added). Fis-induced DNA bending was evaluated by polyacrylamide gel electrophoresis of Fis complexes formed at *proP* P1 (McLeod *et al*., 1999), *rrnB* P1 (Gosink *et al*., 1996; Bokal *et al*., 1997), and *hin*-D (Pan *et al*., 1996). WT indicates the protein-induced DNA bending is similar to that of wild-type Fis; reduced indicates the DNA is approximately 20% less bent (measured at *hin*-D); and more reduced (R71D) indicates a further ~5% reduction in apparent bending angle.

bending as measured by the electrophoretic mobility of Fis-DNA complexes (Pan *et al.*, 1996; Bokal *et al.*, 1997; McLeod *et al.*, 1999).

Amino acid substitutions at specific residues in or near the BC turn region have profound effects on transcriptional activation. The most severe mutants, which display little or no activity, contain changes at Arg71 and Gly72. Transcriptional activation by Q68A and Q74A was reduced by 60-70 % and 70-80 %, respectively. All of the BC turn mutants studied here bind DNA with dissociation constants in the nanomolar range similar to wild-type. However, some of the mutants, including those at positions 71, and 74, form less stable Fis-DNA complexes. We presume that their faster off rates are compensated by faster search rates, perhaps because non-specific intermediate complexes are also destabilized due to the loss of the DNA contact. Nevertheless, the reduced transcriptional activities observed for the mutants whose structures have been determined are not correlated with defects in DNA binding. For example, the poor transcriptional activation by Q74A cannot be compensated *in vitro* by high levels of protein *in vitro*, and Q74A is not defective in activating Hin-catalyzed site-specific DNA inversion. By contrast, the reduced transcriptional activation resulting from mutations at Asn73 may be a result of poor DNA binding as evidenced by the poor overall affinity of N73A for DNA, and the observation that transcriptional activation by N73S is relatively efficient in the presence of high protein concentrations.

Among all of the mutants, Arg71 substitutions show the most varied phenotypes in transcription activation, DNA binding, and DNA bending properties. R71Y promotes similar or higher activation of *proP* P2 and *rrnB* P1 as compared with wild-type, but the Fis-DNA complex is less stable and the DNA is less bent. R71K shows the opposite phenotype in that it down regulates transcription, but the Fis-DNA complex is stable and DNA-bending is normal. R71L, R71A and R71D are defective in transcriptional activation and form less stable DNA complexes with reduced DNA bending. These varied properties suggest that the side-chain of residue 71 is critical for transcriptional activation as well as play a role in DNA binding and bending.

The melting points of all the mutants listed in Table 1 are comparable to that of wild-type, except for G72A and G72D which have melting points 9 to 15 °C lower than that of wild-type Fis. Therefore, the reduced transcriptional activity for most of the mutants does not reflect a decrease in thermal stability. The reduced thermal stability of G72A and G72D suggests that a glycine may be favored at this position for structural reasons (discussed further below). However, the decreased stability of these mutants is probably not responsible for their transcription phenotype because G72A and G72D efficiently activate Hin-catalyzed DNA inversion at 37 °C *in vivo* and *in vitro* (data not shown).

Overall structure of Fis mutants Q68A, G72A, G72D and N74A

Fis mutants Q68A, G72A, G72D and Q74A crystallized in the orthorhombic unit cell isomorphous to that of wild-type Fis. All of the mutant crystals diffracted to ~2.0 Å resolution at −150 °C. Our original wild-type Fis structure was refined to 2.3 Å resolution, and the diffraction data were collected at room temperature (Yuan *et al.*, 1991). In order to obtain a wild-type Fis structure with a comparable resolution to the mutants, a new set of diffraction data for wild-type Fis was collected at −150 °C, and the structure was refined to 2.0 Å resolution (see Table 2). The higher resolution wild-type Fis structure consisted of four α-helices for each monomer from residues 27 to 98. The N-terminal region remained disordered with only eight visible residues (10 to 13 and 23 to 26) located at the bottom of the mobile β-hairpin arm as defined by the structure of the Fis mutant K36E (Safo *et al.*, 1997).

The core structures (residues 27 to 98) of the four mutants are almost identical to that of wild-type Fis, and the N-terminal regions are also mostly disordered in the crystal structures of Fis mutants Q68A, G72A and Q74A (see Figure 3). It is surprising that electron density for one of the β-hairpin arms is visible in G72D with only three residues missing at the tip of the turn. This is the first example where the N-terminal β-hairpin structure has been observed in the wild-type orthorhombic unit cell. This result confirms that the β-hairpin structure, which is mobile and tends to be disordered in crystals but was first revealed in the K36E hexagonal unit cell (Safo *et al.*, 1997), is indeed intrinsic to Fis. In addition, the structures of G72D, G72A, and Q74A revealed residues 5 to 9 in an extended conformation. These residues have not previously been observed in any of the wild-type or mutant Fis structures. Mutational analyses have not identified any biological function for this N-terminal region (residues 1 to 10) (Koch *et al.*, 1991; Osuna *et al.*, 1991), even though it is well conserved among Fis proteins in most enteric bacteria (Beach & Osuna, 1998).

Overall structure of R71Y and R71L

The R71Y and R71L mutants crystallized in orthorhombic unit cells, which were not isomorphous to that of wild-type Fis. Residue Arg71 is one of the primary residues involved in crystal packing in the wild-type orthorhombic unit cell due to its interaction with Tyr69 (O) of the neighboring molecule. The replacement of Arg71 by a Tyr or Leu residue disrupted the original packing and resulted in the formation of crystals with unique unit cells. Crystal structures of R71Y and R71L were solved by the molecular replacement method using the wild-type Fis structure as the searching model. There are two Fis R71Y dimers in an asymmetric unit and eight Fis dimers in one

Table 2. X-ray diffraction statistics for the Fis mutants

	WT	Q68A	R71L	R71Y	G72A	G72D	Q74A
A. *Data collection and processing*							
Space group	$P2_12_12_1$	$P2_12_12_1$	$P2_12_12_1$	$P2_12_12_1$	$P2_12_12_1$	$P2_12_12_1$	$P2_12_12_1$
Cell dimensions	$a = 77.47$	$a = 77.58$	$a = 46.03$	$a = 50.21$	$a = 78.29$	$a = 76.33$	$a = 77.70$
	$b = 50.36$	$b = 50.32$	$b = 70.83$	$b = 57.97$	$b = 50.37$	$b = 50.26$	$b = 50.29$
	$c = 47.70$	$c = 47.53$	$c = 74.69$	$c = 135.30$	$c = 47.26$	$c = 47.91$	$c = 47.34$
Resolution (Å)	2.0	2.1	1.9	2.8	2.0	2.0	1.9
Observed reflections	70,772	46,785	114,334	61,806	61,673	76,866	85,997
Unique reflections	13,174	11,485	19,893	10,232	13,105	12,915	15,224
Completeness-all data (%)	99.7	99.5	99.8	99.5	99.3	99.2	100
Completeness-last shell (%)	99.6	99.3	100	99.8	99.2	98.9	100
(resolution range, Å)	(2.07-2.00)	(2.18-2.10)	(1.97-1.90)	(2.90-2.80)	(2.07-2.00)	(2.07-2.00)	(1.97-1.90)
R_{merge}: all data (%)[a]	6.2	11.4	5.7	10.3	7.4	5.5	7.3
R_{merge}: last shell (%)	25.4	48.2	51.1	51.0	43.6	30.1	55.9
$I/\sigma(I)$: all data	25.0	14.0	30.7	20.2	23.4	31.8	22.7
$I/\sigma(I)$: last shell	6.4	3.1	3.7	4.0	4.6	6.1	3.0
B. *Refinement*							
Resolution range (Å)	20.0-2.0	20.0-2.1	20.0-1.9	20.0-2.8	20.0-2.0	20.0-2.0	20.0-1.9
Reflections	12,853	10,775	19,192	9,915	12,664	12,610	14,597
Non-hydrogen atoms							
Protein	1219	1230	1439	2555	1249	1320	1222
Solvent molecules	117	85	115	69	96	145	101
R-factor (%)[b]	23.3	23.2	22.5	21.6	22.3	23.1	22.3
R_{free} (%)[c]	27.1	27.4	26.0	27.7	26.3	27.9	24.8
Model quality							
r.m.s.d. in							
Bond lengths (Å)	0.011	0.007	0.011	0.008	0.008	0.007	0.009
Bond angles (deg.)	1.082	1.019	1.220	1.015	1.003	1.023	1.074
r.m.s coordinate error (Å)	0.16	0.17	0.15	0.36	0.14	0.09	0.17
(Sigma A)							
Average *B*-factor (Å^2)							
Protein atoms	25.7	21.9	29.9	48.8	28.0	24.6	23.9
Solvent atoms	35.4	28.1	38.7	45.6	35.9	38.0	32.2
Ramachandran plot (%)							
Most favored	93.0	95.4	96.2	90.1	91.3	93.0	95.3
Additionally allowed	7.0	4.6	3.8	9.9	8.3	7.0	4.7
Generously allowed	0	0	0	0	0	0	0
Disallowed	0	0	0	0	0	0	0

[a] $R_{merge} = \Sigma_h\Sigma_i|I_{h,i} - \langle Ih\rangle|/\Sigma_h\Sigma_i I_{h,i}$, where $\langle$Ih$\rangle$ is the mean intensity of the i observations for a given reflection h.
[b] *R*-factor $= \Sigma||F_o| - |F_c||/\Sigma|F_o|$, where $|F_o|$ and $|F_c|$ are the observed and calculated structure-factor amplitudes, respectively.
[c] R_{free} was calculated using a random set 10 % of observations that were omitted during refinement.

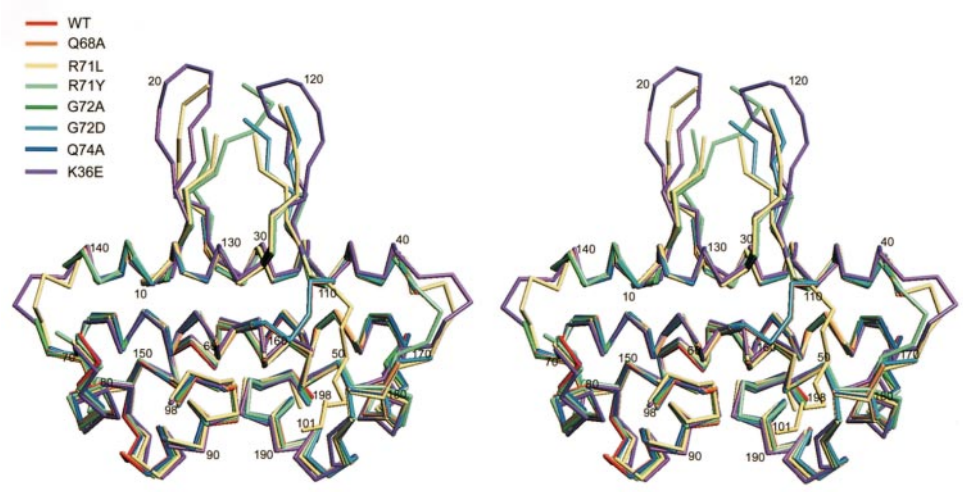

Figure 3. Stereo views of the superimposition of the crystal structures of the wild-type and mutant Fis proteins. All the mutant structures overlap well with that of wild-type Fis in the core domain (residues 27 to 98) with an average rms difference of only 0.5 Å for all the C^{α}-atoms. However, where visible, the N-terminal β-hairpin arms shift significantly, demonstrating the flexibility of this region in solution.

unit cell. The structures of the two asymmetric dimers are almost identical with an rmsd of only 0.5 Å for all the C^{α} atoms. Therefore, only the first dimer was used in the structural comparison described below. The core helix structure (residues 27 to 98) in R71Y is almost identical to that of wild-type Fis with an average rmsd of only 0.5 Å for all the C^{α} atoms. Due to the packing, one of the β-hairpin arms is ordered and its structure is revealed in the electron density map.

In the R71L orthorhombic crystal, there is one dimer per asymmetric unit. The core structure of the final model of R71L is almost identical to that of wild-type Fis with an average rms difference of 0.3 Å for all the C^{α}-atoms in the core region (residues 27 to 98). Unlike most of the mutants, the N-terminal region of the R71L dimer is well defined such that both β-hairpin arms are visible with only a few residues missing at the tips (residues 17-20 and 117-121). Moreover, the N-terminal tail (residues 101 to 110) of one of the R71L subunits is inserted between a pair of β-hairpin arms from the neighboring molecule, resulting in continuous unbroken electron density from the very N-terminal residue (Met 101). Therefore, the crystal structure of R71L offers by far the most complete model of the Fis dimer among all the resolved Fis mutant structures.

Figure 3 shows a combined representation of the backbone structures of each of the BC turn mutants, along with wild-type and K36E (hexagonal form), superimposed over their core (residues 27 to 98) regions. With the exception of the N-terminal regions and the poorly ordered loop between helices A and B, the structures of the backbones are very similar. The positions of the β-hairpin arms as they extend out from the core are shifted in the different crystal forms of K36E, G72D, R71Y, and R71L. This result confirms the earlier suggestion based on cysteine crosslinking studies that the β-hairpin arms are mobile in solution (Safo *et al.*, 1997). The flexibility of the Fis β-hairpin arm region resembles the NMR solution structures of the related HU and TF1 proteins, which also clearly show highly variable positions of the β-arms with respect to the protein core (Jia *et al.*, 1996; Vis *et al.*, 1995). While the Fis β-arms interact with DNA invertases to regulate site-specific inversion, the β-arms of HU interact with DNA. The position of the N-terminal tail in R71L (residues 101 to 109) is different from those of residues 105 to 109 observed in G72D, G72A and Q74A, demonstrating the flexibility of this segment in solution.

The BC turn conformation in the wild-type and mutant Fis proteins are identical

A β-turn is defined as a loop in which the $C^{\alpha}_{i} - C^{\alpha}_{i+3}$ distance is less than 7 Å and the central residues are not helical (Wilmot & Thornton, 1990). The loop between the B and C helices in Fis can be classified as a β-turn because the distance between C^{α} of Thr70 and C^{α} of Asn73 is only 5.4 Å. The φ and ψ angles for Arg71 fall in the region of a left-handed α-helix (α_L), and those of Gly72 fall in a more restricted γ_L region in the Ramachandran plot (see Figure 4). The α_L is located in the left-handed α-helix region centered at (φ, ψ) = (60°, 30°), and γ_L is centered at (φ, ψ) = (90°, 0°). Therefore, the BC turn can be further classified as a type-I′ γγ β-turn. Four hydrogen bonds were observed between main-chain atoms: the carbonyl group of Gln68 and the amino group of Thr70; the carbonyl group of Gln68 and the amino group of Arg71; the carbonyl group of Thr70 and the amino group of Asn73; and the carbonyl group of Gly72 and the amino group of Gln74. The side-chain of Thr70 (OG1) forms two hydrogen bonds with main-chain atoms, the amino and carbonyl groups of Asn73. These hydrogen bond networks, as shown in Figure 5(a), stabilize the BC turn.

The dihedral angles for Gly72 in the γ_L region are quite specific for glycine since other amino acid residues are not normally found in this region (Wilmot & Thornton, 1990). Therefore, mutations of Gly72 cause significant instability in the protein fold as reflected by the decrease of melting points by 9 °C and 15 °C for G72A and G72D, respectively, as compared to wild-type or the other Fis mutants (Table 1). A marked decrease in the melt-

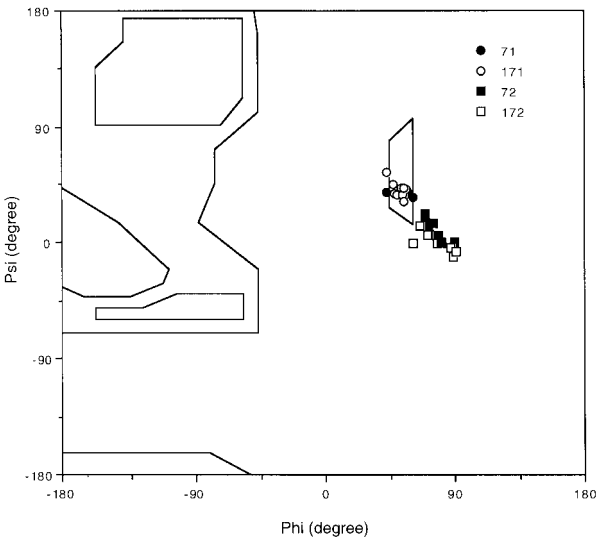

Figure 4. The Ramachandran plot for the residues 71 (or 171 in the second subunit) and 72 (or 172) in the crystal structures of the wild-type Fis and BC turn mutants (Q68A, R71Y, R71L, G72A, G72D, and Q74A). The φ and ψ angles for the Arg71 residues from wild-type Fis fall in the region of a left-handed α-helix (α_L), and those of Gly72 fall in a more restricted γ_L region. The α_L is centered at (φ, ψ) = (60°, 30°), and γ_L is centered at (φ, ψ) = (90°, 0°) in the Ramachandran plot. The φ and ψ angles of residues 71 and 72 from each of the mutants remain in the same regions; in particular, Leu71 and Tyr71 are in α_L, and Ala72 and Asp72 are in γ_L, even though Ala72 and Asp72 are not energetically favored in this region.

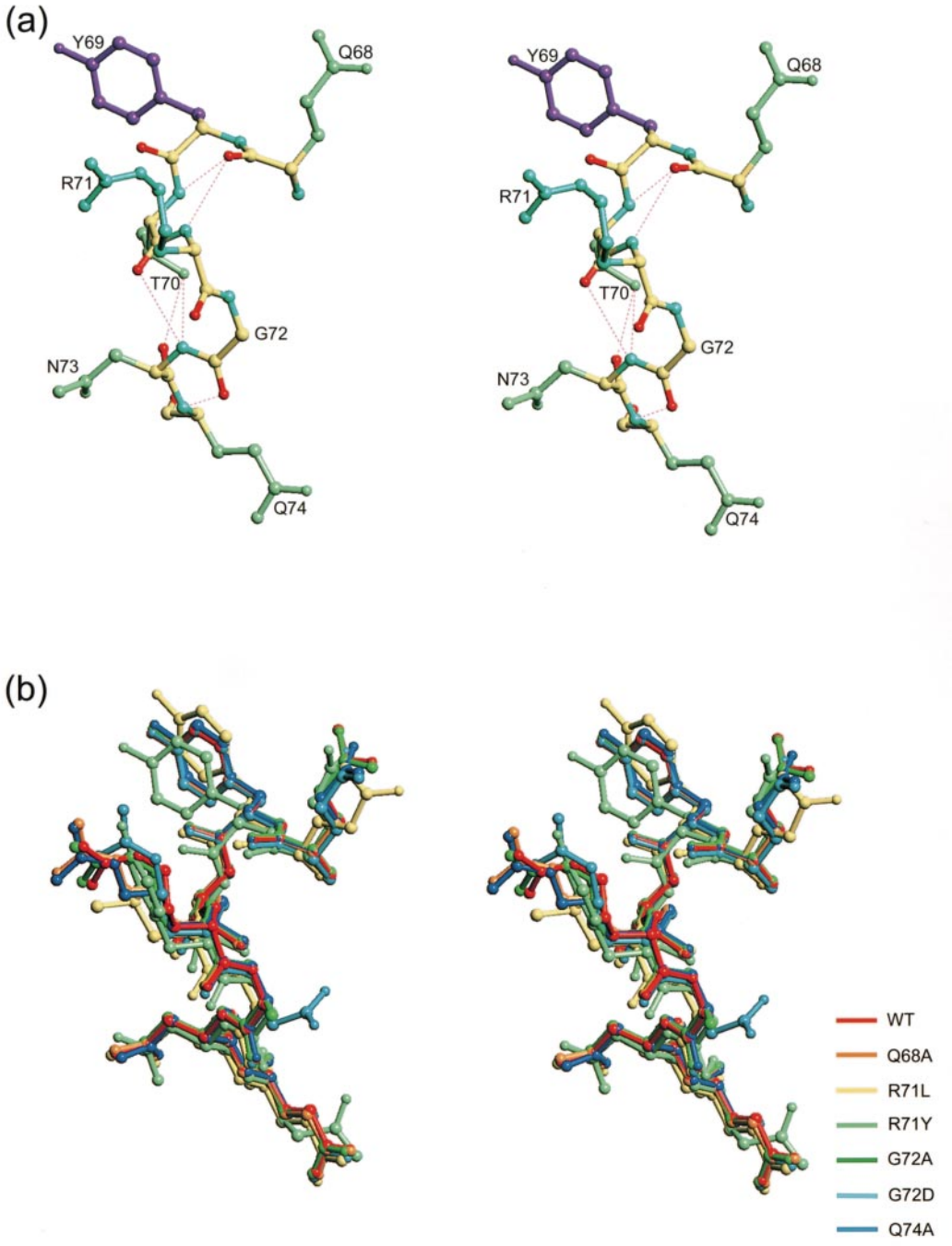

Figure 5. Hydrogen-bond networks in the Fis BC turn and the superimposition of the BC turn in wild-type and mutant Fis proteins. (a) In the wild-type Fis, four hydrogen bonds were observed between the main-chain atoms: Q68 (O)—T70 (NH); Q68 (O)—R71 (NH); T70 (O)—N73 (NH); and G72 (O)—Q74 (NH). The side-chain of T70 (OG1) forms two hydrogen bonds with main-chain atoms, the amino and carbonyl groups of N73. These hydrogen bond networks stabilize the BC turn in Fis. (b) Superimposition of the crystal structures of wild-type and mutant Fis protein shows that the BC turn deviates only slightly in the structures such that the averaged rms difference for the C^{α} atoms (from residues 68 to 74) in the mutants as compared to the wild-type Fis is only 0.6 Å.

ing temperature of Arc repressor was also found when glycine residues (G30A or G49A) located in turn regions were mutated to alanines (Sauer *et al*., 1996). The restricted conformation of the BC turn raised the possibility that the Fis mutant backbone structures within this region might be altered, especially at Gly72, leading to the varied transcriptional activities. However, superimposition of the BC turns of these mutants, as shown in Figure 5(b), demonstrates that the backbone conformation in this region is almost identical for all of the wild-type and mutant Fis proteins. The average rmsd

among all the mutants as compared to wild-type Fis is only 0.3-0.8 Å (Q68A: 0.3 Å; R71L: 0.6 Å; R71Y: 0.8 Å; G72A: 0.3 Å; G72D: 0.4 Å; Q74A: 0.4 Å) for the C^{α} atoms of residues 68 to 74. The higher rmsd for R71L and R71Y are probably the result of the different packing environments in these two mutants as compared to that of wild-type Fis, as well as the lower resolution limit for R71Y (2.8 Å). The ϕ and ψ angles for Leu71 and Tyr71 remain in α_L, and those of Ala72 or Asp72 remain in γ_L, even though an alanine residue or an aspartic acid is not energetically favored in the γ_L region (Figure 4). Moreover, the side-chain of each residue in the BC turn is oriented in a similar way in the mutants as compared with wild-type. Therefore, except for the differences in the side-chains, the conformations of the BC turns in the mutants are almost identical to that of wild-type Fis.

It was noted earlier that the general architecture of the Fis-RNAP activation complex in the *rrnB* P1 resembles the one suggested for CRP-RNAP complex at the *lac* P1 promoter (Bokal *et al*., 1997). A surface loop with a canonical β-turn structure in CRP, from residues 156 to 164, is proposed to interact with the αCTD of RNAP to stimulate transcription of *lac* and other CRP-dependent promoters (Savery *et al*., 1998; Busby & Ebright, 1999). While this β-turn is also located near the N-terminal region of its helix-turn-helix motif, it is more removed from the protein-DNA interface than the BC turn region of Fis. It is interesting that mutations at Gly162 in this β-turn, which falls in a disallowed region in the Ramachandran plot (Parkinson *et al*., 1996), also give one of the strongest phenotypes in transcription activation (Zhou *et al*., 1994). However, the transactivation regions in Fis and CRP are structurally different and the residues involved in protein-protein interactions also share little resemblance; therefore, these two transcription activators may interact with different amino acid residues in αCTD.

Gln74 and Asn73 are likely involved in DNA-binding

In many helix-turn-helix family proteins, a glutamine is the first residue of the first helix in the helix-turn-helix motif and often makes a hydrogen bond to the first residue in the second helix that interacts with the DNA major groove (Brennan, 1991). In wild-type Fis, the side-chain of Gln74 at the N-terminal end of the C-helix is hydrogen bonded to Arg85 (NH2) and Arg89 (NE), which are the first and fifth residues in the D-helix, respectively. Both of these arginine residues are critical for DNA binding and are believed to be contacting bases within the core recognition site (Koch *et al*., 1991; Osuna *et al*., 1991; Pan *et al*., 1996). In addition, Gln74 is thought to contact the DNA phosphate backbone in the Fis-DNA complex, as has been observed with a glutamine at this position in many co-complexes of helix-turn-helix proteins (Pabo *et al*., 1990). The replacement of Gln74 with an alanine residue in Fis abolishes the hydrogen bond network within the protein, as shown in the crystal structure of Q74A, and would be expected to eliminate the DNA phosphate contact in the complex. While Q74A still binds DNA reasonably well, Q74A-DNA complexes display faster dissociation rates, consistent with the loss of hydrogen bonding (Table 1, Pan *et al*., 1996). Therefore, the instability of the protein-DNA complex may contribute to its low transcriptional activation potential. However, mutants such as R71Y display similarly rapid dissociation rates yet efficiently activate transcription, suggesting that the decrease in stability of the Q74A-DNA complex may not be sufficient to fully explain its poor transcription activity. As discussed below, Gln74 also constitutes part of a ridge that includes Gln68, Arg71 and Gly72, which may interact with the αCTD. We conclude that Gln74 may contribute to transcriptional activation by multiple mechanisms.

We have previously argued that Asn73 makes an important contact with DNA due to the poor binding and reduced bending by N73A and the proximity of residue 73 to DNA as probed by attaching the phenanthroline copper DNA cleavage reagent to this position (Pan *et al*., 1994, 1996). Since Asn73 is positioned on the opposite side of the ridge from the other BC turn residues, such as Gln68, Arg71, Gly72 and Gln74, it is likely that the low transcriptional activation by mutations at this residue solely result from their defect in DNA binding. In support of this idea, the low transcription activation promoted by N73S, which binds DNA with greater affinity than N73A, can be largely compensated by adding high amounts of N73S mutant protein to the reaction (McLeod *et al*., 1999).

The molecular surface of the transcriptional activation region in Fis

The molecular surfaces of the transcriptional activation region of wild-type Fis and the BC turn mutants were calculated by GRASP (Nicholl & Honig, 1991) and displayed in Figure 6. Gln68, Arg71, Gly72 and Gln74 form a contiguous protruding surface that we propose contacts the αCTD of RNAP in the activated transcription complex. The side-chain substitutions in each of the transcriptionally-defective mutants causes a change in the surface on one side of this ridge. The change caused by the mutations at Gly72 are particularly informative, since the addition of only a single methyl group on this surface (G72A) is sufficient to essentially abolish activation. The extra methyl group (A72) may directly interfere with the interaction of αCTD. However, we cannot exclude the possibility that binding of αCTD by Fis is accompanied by a conformational change that is only possible with a glycine at this position. The side-chains of Tyr69 and Thr70 (not visible in the Figure), which are not important in transcription since replacement of either of these residues to Ala

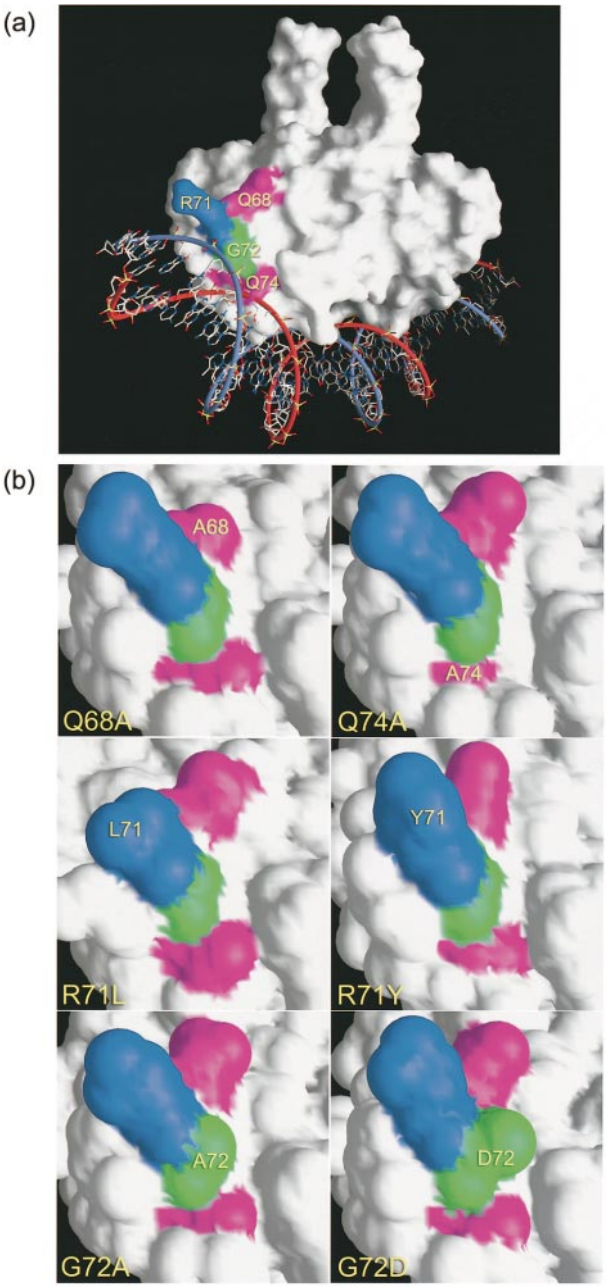

Figure 6. The molecular surface of wild-type and mutant Fis proteins in the BC turn region. (a) Overall molecular surface for the crystal structure of wild-type Fis refined in this study, modeled with a bound DNA (Tzou & Hwang, 1997). Several residues in the BC turn region, Gln68, Arg71, Gly72 and Gln74, are located on a continuous protruding surface adjacent to the helix-turn-helix motif. This ridge is likely to contact the αCTD of RNAP. (b) Molecular surface of the transactivation region of the mutant proteins. The mutated residues are labeled.

causes no effect on transcription (Bokal *et al*., 1997; McLeod *et al*., 1999), extend from the opposite side of this ridge. Residue Asn73 is also located on the other side and, as discussed above, the reduced transcriptional activity for Asn73 is likely a consequence of its poor binding.

The most prominent side-chain on the surface of the BC turn region is that of Arg71, where substitutions lead to the most varied phenotypes in transcriptional activation as well as DNA binding. Previous studies have shown that Arg71 can contact DNA flanking the core Fis-binding site and mediate additional bending within the Fis-DNA complex (Pan *et al*., 1996). Since the guanidinium group of Arg71 contains multiple hydrogen bonding atoms, Arg71 is capable of forming dual interactions with DNA and αCTD. While most amino acid residues at this position strongly decrease transcriptional activation, replacement of Arg71 with aromatic residues leads to mutants that efficiently (R71Y) or partially (R71W and R71F) activate transcription (McLeod *et al*., 1999; S. Aiyar & R. Gourse, personal communication). These results suggest the possibility that Arg71 interacts with αCTD *via* a non-classical amino-aromatic hydrogen bond (Perutz *et al*., 1986) or a classical π-π stacking. In this case, the replacement of Arg71 with an aromatic residue will retain the π-π stacking interaction. A molecular structure of a complex between Fis and αCTD will be required to reveal the precise nature of this interaction.

Experimental Procedures

Protein purification and crystallization

The genes encoding the Fis BC turn mutants (Bokal *et al*., 1997; Gosink *et al*., 1996; McLeod *et al*., 1999) were transferred to pET11a as described by Pan *et al*. (1996). Large-scale preparations of mutant proteins were purified by chromatography on a HiTrap SP column (Pharmacia, Sweden) followed by dialysis against a low salt buffer to precipitate Fis (Osuna *et al*., 1991; Pan *et al*., 1996). Resolubilized Fis was concentrated by centri-plus 3K (Amicon, USA) ultrafiltration and stored at a concentration of 20 mg/ml in 20 mM Tris-HCl (pH 8.2), 1 M NaCl at −70 °C.

Crystals of all the mutants were grown by the hanging drop vapor diffusion method. One microliter of drop solutions containing ~10 mg/ml Fis protein, 1 M NaCl and 20 mM Tris-HCl (pH 8.2), were mixed with 1 μl of reservoir solutions (1 ml) for each mutant. The reservoir solutions for the mutants were: 0.2 M sodium acetate, 0.1 M sodium cacodylate (pH 6.5), and 30 % (w/v) PEG 6000 for Q68A; 0.1 M Na-Hepes (pH 7.5), and 25 % PEG 8000 for R71Y; 0.1 M Na-Hepes (pH 7.5), 2.0 M ammonium sulfate and 2 % PEG 400 for R71L; 0.1 M Na-Hepes (pH 7.5), and 30 % PEG 4000 for G72A; 0.1 M magnesium acetate, 0.1 M sodium cacodylate (pH 6.5), and 20 % PEG 8000 for G72D; 0.2 M sodium acetate, 0.1 M sodium cacodylate (pH 6.5), and 30 % PEG 8000 for Q74A. These conditions gave X-ray diffraction quality crystals after several days at room temperature.

Measurement of the Fis melting points by circular dichroism

The CD spectra were measured at the wavelength of 220 nm on a Jasco J-700 spectropolarimeter in a temperature range varying from 20 to 80 °C at a rate of

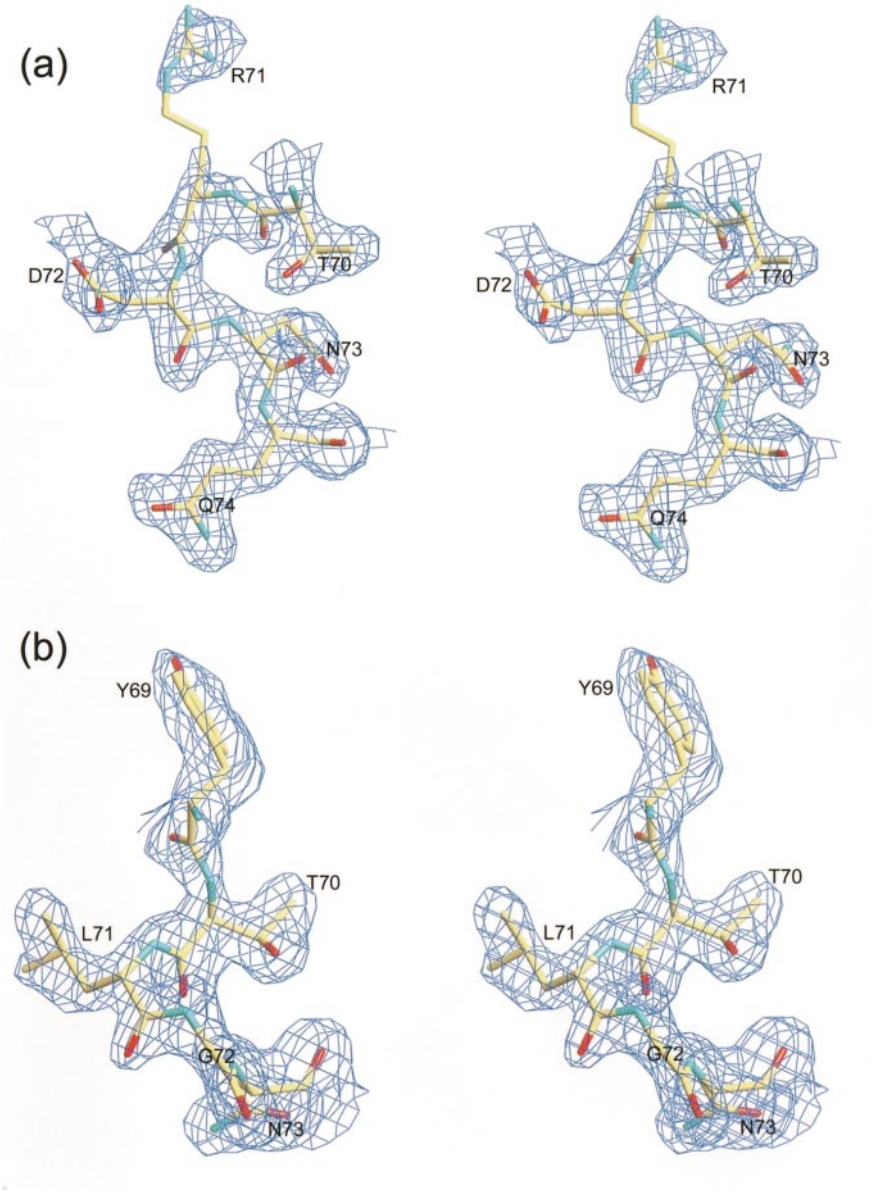

Figure 7. Stereo views of the omitted ($2F_o - F_c$) electron density map of Fis mutants (a) G72D, and (b) R71L superimposed onto the final model in the BC turn region. The map was calculated by omitting the mutated residue and all the atoms within a 3 Å spherical shell, and contoured at 1.0 σ of the average electron density.

50 °C/hour with a NESLAB coolflow controller. The protein concentration was adjusted to 0.02 mg/ml in a buffer solution of 10 mM potassium phosphate at pH 7.5. Thermal denaturation for each mutant was repeated three times, and the measurement results are listed in Table 1.

X-ray Data collection and processing

X-ray diffraction intensities for all the crystals were collected at −150 °C from an R-AXIS II or R-AXIS IV imaging plate system mounted on a Rigaku RU-300 rotating anode equipped with double-focusing mirrors and operated at ~4 kW. All of the Fis mutant crystals were immersed in the cryo-protectant of 10 % (w/v) glycerol and 90 % PEG 8000(30 % (w/v)) for several minutes before data collection. All data sets were integrated, scaled and merged using the HKL program (Otwinowski, 1993), and all the statistics for data collection and processing were summarized in Table 2.

Structure determination for R71Y and R71L

The structure of R71Y was determined by the molecular replacement method with the program XPLOR (Brünger, 1992) using data in the resolution range between 8-4 Å. Two Fis dimers were expected in an asymmetric unit that gave a Matthew's coefficient of 2.2 $Å^3$/Dalton with the corresponding solvent content of 43.6 %. The wild-type Fis dimer structure (PDB accession number: 3FIS) was used as the searching model. The top ten rotation solutions were used for translation search,

and two distinct peaks were identified with correlation coefficients of 26.8 and 23.3 and *R*-factors of 52.1 % and 52.4 %, respectively. Since these two translation solutions may correspond to different origins in the orthorhombic $P2_12_12_1$ unit cell, the relative positions of the two dimers were further determined by cross-translation search with the first molecule fixed and the second one moved by the eight possible half vectors of ($x(\pm 0.5)$, $y(\pm 0.5)$, $z(\pm 0.5)$. A final translation vector of (0, 0.5, 0) was applied to the second molecule and, together with the first one, this initial model gave an *R*-factor of 40.4 % with no bad contacts in packing.

The structure of R71L was also determined by the molecular replacement method using XPLOR. The wild-type Fis dimer structure was used as the searching model and one dimer in an asymmetric unit was expected that gave a Matthew's coefficient of 2.7 Å^3/Dalton and a solvent content of 54.4 %. The highest peak in the rotation function was used for the calculation of translation function with data from 8.0 to 4.0 Å. The highest peak in translation gave a correlation coefficient of 35.8 and an *R*-factor of 46.6 % after rigid body refinement.

Structure refinement

The refinement of all the mutants was carried out using the program CNS (Brünger *et al*., 1998). For cross validation, 10 % of randomly selected data were set aside at the beginning of refinement for the calculation of R_{free} values. Bulk solvent procedure was set up to include low-resolution data between 20 and 8 Å for refinement. All available data ($F > 0$) were used for refinement and calculation of electron density maps. Manual rebuilding of the model and addition of solvent molecules were performed using Turbo-Frodo. In the structures of Q68A, R71L, G72A, G72D, and Q74A, there are two Fis molecules per asymmetric unit, and they are numbered as residues 1 to 98 and 101 to 198. In R71Y, there are four Fis molecules per asymmetric unit, numbered as 1 to 98, 101 to 198, 201 to 298 and 301 to 398, respectively.

The coordinates from our original Fis model (3FIS) (Yuan *et al*., 1991), containing residues 26 to 98 of both subunits and no solvent, was used as the initial model for refinement for the mutants of Q68A, G72A, G72D and Q74A since the crystal forms of these mutants are isomorphous to the wild-type Fis. For R71L and R71Y, the molecular replacement solutions were used as the initial model position for refinement. After initial rigid-body refinement, the structures were further refined for the individual atomic positions and temperature factors. The NCS restraint was applied to the two R71Y dimers in the asymmetric unit during refinement. Manual rebuilding and reciprocal space refinement were performed iteratively. At this stage, the *R*-factors for all of the mutants were below 30 % and the electron density maps were examined closely at the N-terminal region and peptide fragments were assigned to the Fourier map if they were interpretable. The residues in the loop between helices A and B often lacked well-defined densities and as a consequence, were omitted from the model. The mutated residues in all of the mutants gave a well-defined density, and the omitted electron density map for two of the mutants, G72D and R71L, is displayed in Figure 7. The NCS restraint for R71Y was removed at the final stage of the refinement. The final model of Q68A contains: residues 9 to 13, 25 to 42, 47 to 98, 105 to 113, 125 to 141, 146 to 198 and 85 water molecules; R71L: residues 9 to 16, 21 to 98, 101 to 116, 122 to 198 and 115 water molecules; R71Y: residues 10 to 19, 22 to 42, 45 to 98, 110 to 114, 124 to 141, 146 to 198, 201 to 213, 225 to 298, 310 to 314, 323 to 398 and 69 water molecules; G72A: residues 9 to 13, 25 to 42, 47 to 98, 105 to 113, 125 to 141, 145 to 198 and 96 water molecules; G72D: residues 9 to 14, 25 to 42, 47 to 98, 105 to 117, 121 to 141, 145 to 198, and 145 water molecules; Q74A: residues 10 to 13, 25 to 42, 47 to 98, 105 to 113, 125 to 141, 146 to 198 and 101 water molecules. Refinement statistics are listed in Table 2.

Protein Data Bank accession codes

The accession codes for each of the mutants in the RCSB Protein Data Bank are 1ETY (WT), 1ETK (Q68A), 1ETO (R71L), 1ETQ (R71Y), 1ETV (G72A), 1ETW (G72D), and 1ETX (Q74A).

Acknowledgments

We thank Leah Corselli for subcloning of the Fis mutant genes, Tzu-Ping Ko for early contributions to the project, and Sarah McLeod and Stacy Merickel for comments on the manuscript. We also thank Sarah Aiyar and Richard Gourse for discussion and unpublished data of Fis mutant activities on *rrnB* P1 transcription. This work was supported in part by the Foundation of Biomedical Sciences and National Science Council grants to H. S. Y. (NSC 88-2311-B-001-109 and NSC 89-2320-B-001-014), and NIH grant GM38509 to R. C. J.

References

Ali Azam, T., Iwata, A., Nishimura, A., Ueda, S. & Ishihama, A. (1999). Growth phase-dependent variation in protein composition of the *Escherichia coli* nucleoid. *J. Bacteriol.* **181**, 6361-6370.

Ball, C. A., Osuna, R., Ferguson, K. C. & Johnson, R. C. (1992). Dramatic changes in Fis levels upon nutrient upshift in *Escherichia coli*. *J. Bacteriol.* **00**, 8043-8056.

Beach, M. B. & Osuna, R. (1998). Identification and characterization of the *fis* operon in enteric bacteria. *J. Bacteriol.* **180**, 5932-5946.

Bokal, A. J., Ross, W. & Gourse, R. L. (1995). The transcriptional activator protein FIS: DNA interactions and cooperative interactions with RNA polymerase at the *Escherichia coli rrnB* P1 promoter. *J. Mol. Biol.* **245**, 197-207.

Bokal, A. J., Ross, W., Gaal, T., Johnson, R. C. & Gourse, R. L. (1997). Molecular anatomy of a transcription activation patch: Fis-RNA polymerase interactions at the *Escherichia coli rrnB* P1 promoter. *EMBO J.* **16**, 154-162.

Brennan, R. G. (1991). Interactions of the helix-turn-helix binding domain. *Current Opin. Struct. Biol.* **1**, 80-88.

Brünger, A. T. (1992). *X-PLOR, version 3.1: a system for X-ray Crystallography and NMR*, Yale University Press, New Haven, CT.

Brünger, A. T., Adams, P. D., Clore, G. M., Delano, W. L., Gros, P. & Grosse-Kunstleve, R. W., *et al*. (1998). Crystallography and NMR System (CNS): a new software system for macromolecular structure determination. *Acta Crystallog. sect. D*, **54**, 905-921.

Busby, S. & Ebright, R. H. (1999). Transcription activation by catabolite activator protein (CAP). *J. Mol. Biol.* **293**, 199-213.

Champagne, N. & Lapointe, J. (1998). Influence of FIS on the transcription from closely spaced and non-overlapping divergent promoters for an aminoacyl-tRNA synthetase gene (*gltX*) and a tRNA operon (*valU*) in *Escherichia coli*. *Mol. Microbiol.* **27**, 1141-1156.

Falconi, M., Brandi, A., La Teana, A., Gualerzi, C. O. & Pon, C. L. (1996). Antagonistic involvement of FIS and H-NS proteins in the transcriptional control of *hns* expression. *Mol. Microbiol.* **19**, 965-975.

Gonzalez-Gil, G., Bringmann, P. & Kahmann, R. (1996). FIS is a regulator of metabolism in *Escherichia coli*. *Mol. Microbiol.* **22**, 21-29.

Gosink, K. K., Gaal, T., Bokal, A. J., IV & Gourse, R. L. (1996). A positive control mutant of the transcription activator protein Fis. *J. Bacteriol.* **178**, 5182-5187.

Green, J., Anjum, M. F. & Guest, J. R. (1996). The ndh-binding protein (Nbp) regulates the *ndh* gene of *Escherichia coli* in response to growth phase and is identical to Fis. *Mol. Microbiol.* **20**, 1043-10055.

Hochschild, A. & Dove, S. L. (1998). Protein-protein contacts that activate and repress prokaryotic transcription. *Cell,* **92**, 597-600.

Ishihama, A. (1993). Protein-protein communication within the transcription apparatus. *J. Bacteriol.* **175**, 2483-2498.

Jia, X., Grove, A., Ivancic, M., Hsu, V. L., Geiduschek, E. P. & Kearns, D. R. (1996). Solution structure of the *Bacillus subtilis* phage SP01-encoded type II DNA-binding protein TF1 in solution. *J. Mol. Biol.* **263**, 259-268.

Johnson, R. C., Bruist, M. F. & Simon, M. I. (1986). Host protein requirements for *in vitro* site-specific DNA inversion. *Cell,* **46**, 531-539.

Koch, C. & Kahmann, R. (1986). Purification and properties of the *Escherichia coli* host factor required for inversion of the G segment in bacteriophage Mu. *J. Biol. Chem.* **261**, 15673-15678.

Koch, C., Ninnemann, O., Fuss, H. & Kahmann, R. (1991). The N-terminal part of the *E. coli* DNA binding protein Fis is essential for stimulating site-specific DNA inversion but is not required for specific DNA binding. *Nucl. Acids Res.* **19**, 5915-5922.

Kostrewa, D., Granzin, J., Koch, C., Choe, H.-W., Raghunathan, S., Wolf, W., Kahmann, R. & Saenger, W. (1991). Three-dimensional structure of the *E. coli* DNA-binding protein Fis. *Nature,* **349**, 178-180.

Lazarus, L. R. & Travers, A. A. (1993). The *Escherichia coli* FIS protein is not required for the activation of *tyrT* transcription on entry into exponential growth. *EMBO J.* **12**, 2483-2494.

McLeod, S. M., Xu, J., Cramton, S. E., Gaal, T., Gourse, R. L. & Johnson, R. C. (1999). Localization of amino acids required for Fis to function as a class II transcriptional activator at the RpoS-dependent *proP* P2 promoter. *J. Mol. Biol.* **294**, 333-346.

McLeod, S. M., Xu, J. & Johnson, R. C. (2000). Co-activation of the RpoS-dependent *proP* promoter by Fis and CRP. *J. Bacteriol.* **182**, 4180-4187.

Nicholl, A. & Honig, B. J. (1991). A rapid finite difference algorithm utilizing successive over-relaxation to solve the Poisson-Boltzman equation. *J. Comput. Chem.* **12**, 435-445.

Nilsson, L., Vanet, A., Vijgenboom, E. & Bosch, L. (1990). The role of Fis in trans-activation of stable RNA operons of *E. coli*. *EMBO J.* **9**, 727-734.

Osuna, R., Finkel, S. E. & Johnson, R. C. (1991). Identification of two functional regions in Fis: the N terminus is required to promote Hin-mediated DNA inversion but not lambda excision. *EMBO J.* **10**, 1593-1603.

Osuna, R., Lienau, D., Hughes, K. T. & Johnson, R. C. (1995). Sequence, regulation, and functions of *fis* in *Salmonella typhimurium*. *J. Bacteriol.* **177**, 2021-2032.

Otwinowski, Z. (1993). Oscillation data reduction program. In *Proceedings of the CCP4 Study Weekend: Data Collection and Processing* (Sawyer, L., Isaacs, N. & Bailey, S., eds), pp. 56-62, SERC Daresbury Laboratory, Warrington, UK.

Pabo, C. O., Aggarwal, A. K., Jordan, S. R., Beamer, L. J., Obeysekare, U. R. & Harrison, S. C. (1990). Conserved residues make similar contacts in two repressor-operator complexes. *Science,* **247**, 1210-1213.

Pan, C. Q., Feng, J.-A., Finkel, S. E., Landgraf, R., Sigman, D. & Johnson, R. C. (1994). Structure of the *Escherichia coli* Fis-DNA complex probed by protein conjugated with 1,10-phenanthroline copper(I) complex. *Proc. Natl Acad. Sci, USA,* **91**, 1721-1725.

Pan, C. Q., Finkel, S. E., Cramton, S. E., Sigman, D. S. & Johnson, R. C. (1996). Variable structures of Fis-DNA complexes determined by flanking DNA contacts. *J. Mol. Biol.* **264**, 675-695.

Parkinson, G., Wilson, C., Gunasekera, A., Ebright, Y. W., Ebright, R. E. & Berman, H. M. (1996). Structure of the CAP-DNA complex at 2.5 Å resolution: a complete picture of the protein-DNA interface. *J. Mol. Biol.* **260**, 395-408.

Perutz, M. F., Fermi, G., Abraham, D. J., Poyart, C. & Busaux, E. J. (1986). Hemoglobin as a receptor of drugs and peptides: X-ray studies of the stereochemistry of binding. *J. Am. Chem. Soc.* **108**, 1064-1078.

Rhodius, V. A. & Busby, S. J. W. (1998). Positive activation of gene expression. *Curr. Opin. Microbiol.* **1**, 152-159.

Ross, W., Thompson, J. F., Newlands, J. T. & Gourse, R. L. (1990). *E. coli* Fis protein activates ribosomal RNA transcription *in vitro* and *in vivo*. *EMBO J.* **9**, 3733-3742.

Safo, M. K., Yang, W. Z., Corselli, L., Cramton, S. E., Yuan, H. S. & Johnson, R. C. (1997). The transactivation region of the Fis protein that controls site-specific DNA inversion contains extended mobile β-hairpin arms. *EMBO J.* **16**, 6860-6873.

Sauer, R. T., Milla, M. E., Waldburger, C. D., Brown, B. M. & Schildbach, J. F. (1996). Sequence determinants of folding and stability for the P22 Arc repressor dimer. *FASEB,* **10**, 42-48.

Savery, N. J., Lloyd, G. S., Kainz, M., Gaal, T., Ross, W., Ebright, R. E., Gourse, R. L. & Busby, S. J. W. (1998). Transcription activation at class II CRP-dependent promoters: identification of determinants in the C-terminal domain of the RNA polymerase α subunit. *EMBO J.* **17**, 3439-3447.

Tzou, W.-S. & Hwang, M.-J. (1997). A model for Fis N terminus and Fis-invertase recognition. *FEBS Letters,* **401**, 1-5.

Vis, H., Mariani, M., Vorgias, C. E., Wilson, K. S., Kaptein, R. & Boelens, R. (1995). Solution structure of the HU protein from *Bacillus stearothermophilus*. *J. Mol. Biol.* **254**, 692-703.

Wilmot, C. M. & Thornton, J. M. (1990). β-Turns and their distortions: a proposed new nomenclature. *Protein Eng.* **3**, 479-493.

Wu, H., Tyson, K. L., Cole, J. A. & Busby, S. L. (1998). Regulation of transcription initiation at the *Escherichia coli nir* operon promoter: a new mechanism to account for co-dependence on two transcription factors. *Mol. Microbiol.* **27**, 493-505.

Xu, J. & Johnson, R. C. (1995a). Identification of genes negatively regulated by Fis: Fis and RpoS comodulate growth-phase-dependent gene expression in *Escherichia coli*. *J. Bacteriol.* **177**, 938-947.

Xu, J. & Johnson, R. C. (1995b). Fis activates the RpoS-dependent stationary-phase expression of *proP* in *Escherichia coli*. *J. Bacteriol.* **177**, 5222-5231.

Xu, J. & Johnson, R. C. (1997). Activation of RpoS-dependent *proP* P2 transcription by the Fis protein *in vitro*. *J. Mol. Biol.* **270**, 346-359.

Yuan, S. H., Finkel, S. E., Feng, J. A., Kaczor-Grezskowiak, M., Johnson, R. C. & Dickerson, R. E. (1991). The molecular structure of wild-type and a mutant Fis: relationship between mutational changes and recombinational enhancer function or DNA bending. *Proc. Natl Acad. Sci. USA,* **88**, 9558-9562.

Zhou, Y., Merkel, T. J. & Ebright, R. H. (1994). Characterization of the activating region of *Escherichia coli* catabolite gene activator protein (CAP) II. Role at Class I and Class II CAP-dependent promoters. *J. Mol. Biol.* **243**, 603-610.

Edited by R. Huber

(Received 18 May 2000; received in revised form 18 August 2000; accepted 18 August 2000)